

Reducing aircraft radar cross-section with owl wing type serrated trailing edges

T. Sai Teja, Manoj B. Vaghela and Avijit Chatterjee*

Department of Aerospace Engineering, Indian Institute of Technology Bombay, Mumbai 400 076, India

Serrations at trailing edges of aircraft wing have long been known to suppress flow noise by suitably altering the flow at the trailing edge. Serrations at trailing edges are now also being used to reduce surface edge return contribution in scattering of electromagnetic waves by combat aircraft wing in order to reduce detectability by radar. A study was carried out on the efficacy of trailing edge serrations found in the wing of a barn owl, formed by its primary remiges or flight feathers, towards minimizing trailing edge related contributions by a common combat aircraft wing in an electromagnetic field. The barn owl is especially well known for its silent flight which is usually attributed to multiple adaptations in its wings including at the trailing edge. Barn owl type trailing edge serrations are appended to a planar metallic delta wing and subjected to an incident electromagnetic field. Electromagnetic scattering is predicted by numerically solving Maxwell's equations using a finite volume time domain method and the radar cross-section calculated.

Keywords: Barn owl, finite volume time domain, Maxwell's equations, radar cross-section, stealth, serrations.

THE barn owl is a nocturnal bird of prey famous for its silent stealthy flight. The hushed flight of the barn owl is attributed to its low speed flight and special noise mitigating properties of its wings. The low speed flight of the barn owl is enabled by aerodynamic features like low wing loading and large wing section camber. Special noise reduction mechanisms identified in the barn owl wing are comb-like serrations at the wing leading edge, soft upper surface texture and fringes at the wing trailing edge (TE)¹. Trailing and leading edge adaptations in the barn owl wing have been attempted to be replicated for noise reduction in aircraft wings and wind turbines². The much finer TE fringes in a barn owl wing get attached to TE serrations formed by its primary and secondary remiges^{2,3}. It is the serrations at wing TEs that has classically been the focus of many studies on noise reduction. The reduction in flow noise due to serrations at a wing TE is usually attributed to reducing the effective wing span contributing to noise generation⁴ and to an efficient regrouping of flow leaving the upper and lower surfaces

of the wing leading to a reduced strength of vorticity shed at the TE⁵.

Stealth flight in the case of modern combat aircraft is mostly obtained by controlling the scattering of electromagnetic (EM) waves when it is illuminated by EM field due to radar. Reducing the radar cross-section (RCS), the quantitative measure of detectability due to radar, is an important element in the design of modern combat aircraft. Major techniques involved in reducing RCS include shaping the configuration to deflect EM returns away from the receiver, employing radar absorbing materials (RAM) and use of serpentine intakes. Contribution of edge return to the backscatter or RCS due to the presence of surface discontinuity in targets like aircraft and missiles can become significant when the more dominant specular scattering is reduced or almost nullified by effective shaping. The form of surface discontinuity and orientation of the incident wave, play a major role in the distribution of the scattered field or the bistatic RCS away from the target in case of edge returns involving surface traveling waves⁶. In general the geometric manipulation of wing leading and trailing edges can lead to further reduction in overall RCS of aircraft by reducing the contribution of edge returns. Serrations at wing TE in some form have classically used in various low observable or stealth aircraft configurations like B-2 and F-117A and continue to play an important part in the conceptual design of fifth generation fighter aircraft. Reduction in RCS due to serrations at wing TE, like that for noise control, is usually attributed to reduction in effective spanwise edge length, damping and redirecting away from receiver of the edge diffracted EM waves at the TE.

A computational study was carried out on the effect of using TE serrations, typical of a barn owl wing, in reducing RCS of a common combat wing configuration. Barn owl wing type TE serrations were appended to the TE of a planar metallic delta wing, and the effect on the RCS predicted with the target immersed in a time harmonic EM field. The computational technique requires solving 3D Maxwell's equations in the time domain using a finite volume time domain (FVTD) method^{7,8}. The FVTD method in the present study used an unstructured discretization allowing for greater flexibility in dealing with non-uniform TE serrations typical of barn owl wing in the computational framework.

Electromagnetic scattering from a planar metallic delta wing with TEs that are unserrated, triangular serrated and similarly serrated to that in a barn owl wing were studied for various incidence angles in the wing longitudinal or pitch plane at three different frequencies and electric sizes. Previous studies⁹ have shown TE serrations in a planar delta wing to be ineffective in edge scattering suppression for incidence angles away from nose-on in the wing yaw plane. Figure 1 shows the geometry of the planar delta wing without serrations at the TE. This geometry is identical to that used earlier^{9,10} and has a span of

*For correspondence. (e-mail: avijit@aero.iitb.ac.in)

480 mm which is approximately 4λ , 8λ and 16λ at frequencies of 2.5, 5 and 10 GHz respectively, used in the current study, where λ is wavelength of the incident harmonic wave propagating in \mathbf{K} direction. Figure 2a shows the same planform with triangular serrations. The included angle is 114° and the serrated edge length measures 71.54 mm which is approximately 0.6λ , 1.2λ and 2.4λ respectively, at frequencies specified above. This delta wing with triangular serrated TE was also studied earlier^{9,10}, and results in a relatively substantial 10 dB reduction in RCS in this frequency range over the original planform. TE configurations shown in Figure 2b and c resemble the natural shapes of barn owl wings^{2,3}. The flight feathers in a barn owl wing can be grouped into outer primary remiges and inner secondary remiges. TE serrations are relatively more prominent due to primary remiges which are approximately 10 in number in a single wing^{2,3}. TE configurations shown in Figure 2b and c are obtained by accommodating approximately 10 serrations over half-span of the delta wing to mimic serrations due to primary remiges in an actual barn owl wing. As in the case of the barn owl the serrations also tend to be non-uniform and more prominent in the wing tip region compared to wing root. The configuration in Figure 2b has typical TE serrations found in a barn owl wing^{2,3},

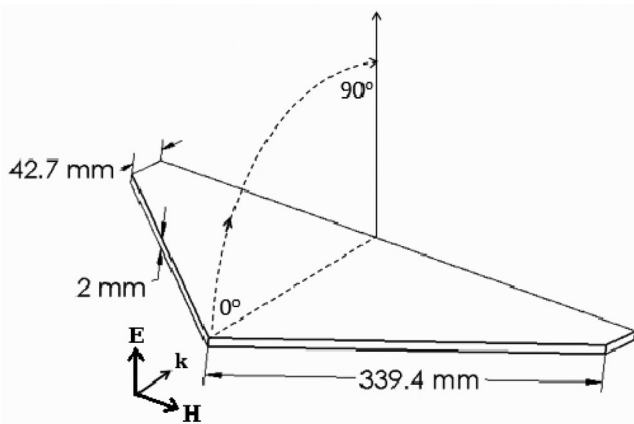


Figure 1. Delta wing without serrations.

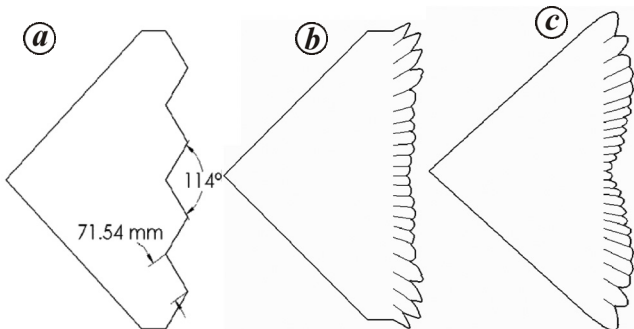


Figure 2. Wing planform with trailing edge serrations. a, Triangular; b, Barn Owl – 1; c, Barn Owl – 2.

appended to a normal TE, whereas that in Figure 2c has it extended on to the tip region. In Figure 3, TE serrations for the three cases are superimposed on the unserrated TE. The average height of the barn owl type TE serrations measured from respective zero-serration lines AB and A'B' in Figure 3, approximates the height h of the triangles forming to triangular serrations. Configurations with barn owl type TE serrations can offer relatively larger wing area compared to triangular serrations. Wing area of the delta wing with first and second type of barn owl TE serrations is approximately 1.05 and 1.22 times respectively, that of wing with triangular TE serrations.

The FVTD^{7,8} method which solves the time-domain Maxwell's equations in integral form on 3D unstructured meshes using a method of lines approach is used to predict electromagnetic scattering and the resulting RCS. The scattered field resulting from an incident sinusoidal EM field is solved. The flux formulation used in spatial discretization is based on a flux-splitting method and provides for second-order spatial accuracy⁷. The wing surface is considered to be metallic and a perfect electric conductor. The far-field boundary has absorbing boundary conditions and temporal evolution is through a two-stage Runge–Kutta method. The time harmonic steady state results obtained are Fourier-transformed to obtain complex surface currents, which in-turn, are then used to obtain RCS values in the far-field¹¹. The present FVTD code has been extensively validated for widely accepted benchmark low-observable targets like NASA almond, ogive, cone-sphere, etc.¹². To further verify the code for delta wing type configurations as in the present study,

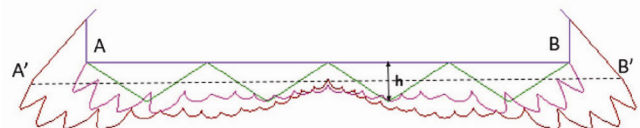


Figure 3. Serrations with respect to plain trailing edge.

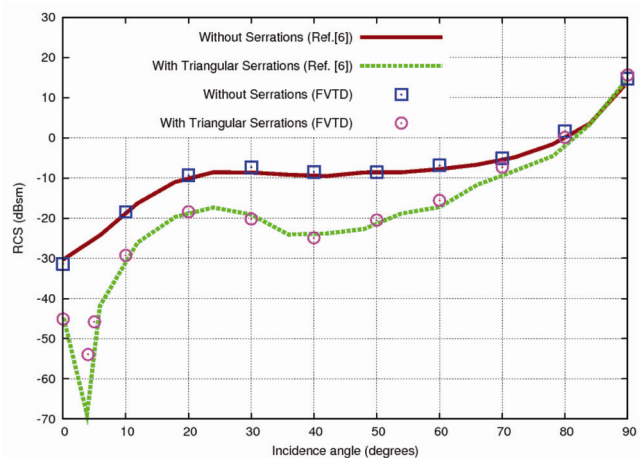


Figure 4. Comparison of monostatic RCS with literature.

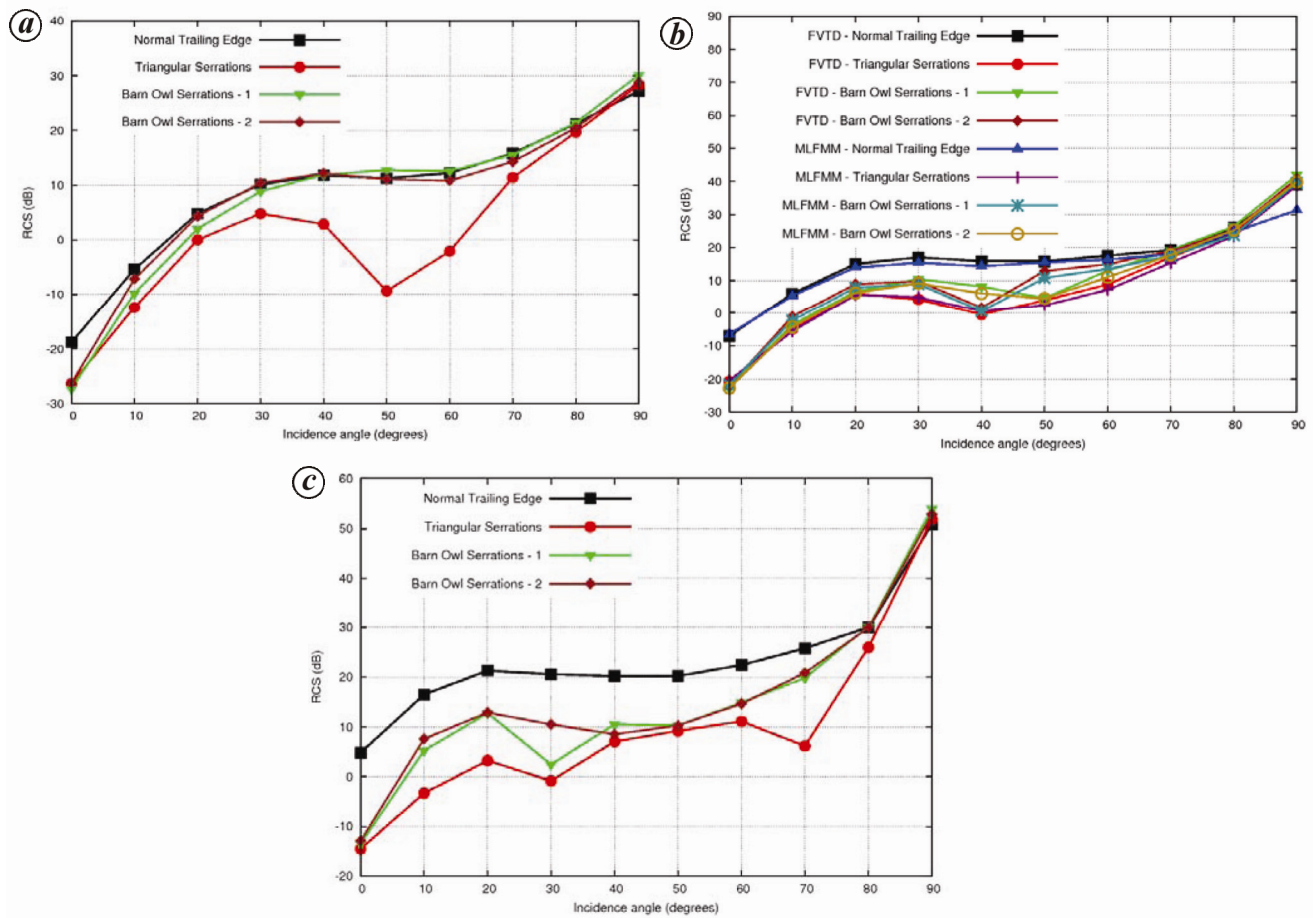


Figure 5. Monostatic RCS with varying incidence (vertical polarization). *a*, 2.5 GHz; *b*, 5 GHz; *c*, 10 GHz.

RCS is computed for the chosen delta wing with and without triangular serrations at 5 GHz for vertical polarization in the wing pitch plane and results are compared with those in the literature¹⁰. The surface mesh of the wing is generated with 35 points per-wavelength (PPW) resolution. The volume mesh consists of approximately 2 million tetrahedron elements. Figure 4 compares computed monostatic RCS with reference data in the literature. It can be seen that there is good agreement between the computed and reference values in the literature.

Surface meshes for the delta wing with different TE configurations, described in Figure 2, are also generated with approximately 35 PPW for the three different frequencies of 2.5, 5 and 10 GHz. Surface travelling waves which contribute to edge return are considered significant when the incident electric field has a component perpendicular to the surface and in the plane of incidence⁶. In the case of a planar delta wing this holds true only for vertically polarized incident waves in the wing pitch plane, as in Figure 1, for which results are presented. Incidence angle 0° indicates nose-on direction while 90° indicates broadside incidence as shown in Figure 1. The RCS values are normalized with respect to λ^2 . Figure 5

compares the monostatic RCS at different incidence angles for vertical polarization incident harmonic waves at frequencies of 2.5, 5 and 10 GHz. It can be observed that RCS is reduced by up to 10–20 dB for the important nose-on incidence for all the serrated TE configurations considered. At higher frequencies, this reduction is more significant as the electrical size of the TE serrations increases. The electrical size is defined with respect to the incident wavelength. In Figure 5 *b*, an additional verification of results is presented by comparing FVTD results with that obtained independently using the frequency domain based multilevel fast multipole method (MLFMM). With the increase in incidence angle away from nose-on, the triangular serrations result in relatively larger RCS reduction at all frequencies compared to the barn owl type TE configurations. But at higher frequencies of 10 GHz, barn owl configurations start becoming competitive for intermediate incidence angles between 0° and 90° with an average reduction up to 10 dB. This is again due to increase in electrical size of TE serrations in the barn owl configurations with decrease in incident wavelength. It may also be noted that the delta wing with barn owl type serrations can have a relatively larger wing

area compared to that of the more conventional triangularly serrated TE wing with identical zero-serration TE lines.

TE serrations formed by primary remiges in a barn owl wing which typically contributes to noise suppression, were appended to a planar metallic delta wing, and used to reduce edge return contributions to the backscatter due to the interaction of surface traveling waves with the wing TE in an electromagnetic field. Results indicate the efficacy of barn owl type TE serration in reducing the RCS of the host delta wing especially in the crucial nose-on incidence. These serrations also become effective away from nose-on incidences with an increase in electrical size arising from decrease in the incident wavelength of incident harmonic wave. The present study indicates more optimized TE serrations inspired by that evolved for bird of prey like the barn owl for silent flight, may be able to RCS of aircraft wing in an EM field, while maintaining higher wing area for superior aerodynamic performance of the host configuration compared to more conventional serrations.

1. Lilley, G. M., *A Study of the Silent Flight of the Owl*, AIAA Paper 1998-2340, 1998.
2. Bachmann, T. and Wagner, H., The three-dimensional shape of serrations at barn owl wings: towards a typical natural serration as a role model for biomimetic applications. *J. Anat.*, 2011, **2**, 192–202.
3. Bachmann, T., Klan, S., Baumgartner, W., Klass, M., Schroder, W. and Wagner, H., Morphometric characterisation of wing feathers of the barn owl *Tyto alba pratincola* and the pigeon *Columba livia*. *Front. Zool.*, 2007, **4**, 192–202.
4. Howe, M., Aerodynamic noise of a serrated trailing edge. *J. Fluids Struct.*, 1991, **5**, 33–45.
5. Moreau, D. J. and Doolan, C. J., Noise-reduction mechanism of a flat-plate serrated trailing edge. *AIAA J.*, 2013, **51**, 2513–2522.
6. Knott, E. F., Shaeffer, J. and Tuley, M., *Radar Cross Section*, SciTech Publishing, Institution of Engineering and Technology, Electromagnetics and Radar Series, 2004, 2nd edn.
7. Bonnet, P., Ferrieres, X., Michielsen, B. L., Klotz, P. and Roumiguieres, J. L., Finite-volume time domain method, In *Time Domain Electromagnetics* (ed. Rao, S. M.), Academic Press Series in Engineering, 1999, pp. 307–367.
8. Chatterjee, A. and Shrial, A., Essentially non-oscillatory finite volume scheme for electromagnetic scattering by thin dielectric coatings. *AIAA J.*, 2004, **42**, 361–365.
9. Chen, H.-Y., Deng, L.-J., Zhou, P.-H. and Xie, J.-L., Tapered impedance loading for suppression of edge scattering. *IET Microwaves, Antennas Propagation*, 2011, **5**, 1744–1749.
10. Lu, L.-J., Chen, H.-Y., Zhou, P.-H., Liang, D.-F. and Deng, L.-J., Design of controlling edge scattering based on tapered periodic surfaces loading. In *Proceedings of Progress in Electromagnetics Research Symposium*, Guangzhou, China, 2014.
11. Balanis, C. A., *Advanced Engineering Electromagnetics*, John Wiley, 1989, pp. 285–291.
12. Woo, A. C., Wang, H. T. G. and Schuh, M. J. and Sanders, M. L., EM Programmer's Notebook – Benchmark radar targets for the validation of computational electromagnetics programs. *IEEE Antenn. Propag. Magazine*, 1993, **35**, 84–89.

Received 11 April 2016; revised accepted 12 November 2016

doi: 10.18520/cs/v112/i05/1020-1023

Indigenous development of a millikelvin refrigerator at VECC, Kolkata

Nisith Kr. Das*, Jedidiah Pradhan, Bidhan Ch Mondal, Anindya Roy, Z. A. Naser and Pradeep Kumar

Variable Energy Cyclotron Centre, 1/AF, Bidhan Nagar, Kolkata 700 064, India

Technologies related to production of millikelvin temperature have been developed and tested in the laboratory. All the critical components were assembled to make a complete dilution refrigerator. The refrigerator was successfully run and commissioned in VECC. The system involves several advanced cryogenic concepts especially the capillary impedance and heat exchanger. A temperature to the tune of 50 mK has been achieved. This is the first development of its kind in India, and likely to usher a new wave in the research arena of advanced cryogenics.

Keywords: Evaporator, mixing chamber, Millikelvin, ^3He – ^4He mixture.

VARIABLE Energy Cyclotron Centre (VECC), Kolkata, has been pursuing several important cryogenic activities over the years, viz. development of superconducting magnet for cyclotron, superconducting magnetic energy storage (SMES), cryogen-free magnets, and superconducting RF cavities and technologies for very low temperature systems. Recently, the Centre has indigenously designed, developed and tested a dilution refrigerator for producing millikelvin temperature. Initially, the project was aimed at developing technologies relevant to dilution refrigerator; all components were designed, developed and tested in the laboratory and finally assembled to make a complete dilution refrigerator as shown in Figure 1.

Helium evaporation is an important cooling technique. The lowest temperature is limited by vapour pressure. Since vapour pressure decreases exponentially with falling temperature, cooling by evaporation of ^4He liquid can only reach about 1 K temperature. Below this temperature, the vapour is very small, and very little would evaporate. Because of the lower mass of the atom, ^3He has higher vapour pressure and therefore higher vaporization rate. Hence, we can reach further down to 0.3 K if we use ^3He instead of ^4He . Cooling below 0.3 K is not possible by conventional refrigeration technique; however, a dilution refrigerator can cool down to a few mK that can be maintained for several hours. It is based on the solution and separation of two isotopes of helium, ^3He

*For correspondence. (e-mail: nkdas@vecc.gov.in)